Available online at www.sciencedirect.com
ScienceDirect
Cement and Concrete Research 37 (2007) 1524–1530
Cement and Concrete Research

Quantitative mineralogical analysis of hydraulic limes by X-ray diffraction

G. Mertens [a,*], P. Madau [b], D. Durinck [c], B. Blanpain [c], J. Elsen [a]

[a] Fysico-chemische Geologie, Katholieke Universiteit Leuven, Celestijnenlaan 200E, 3001 Heverlee, Belgium
[b] Chimie Industrielle, Université Libre de Bruxelles, avenue F.D. Roosevelt 50, 1050 Bruxelles, Belgium
[c] MTM, Katholieke Universiteit Leuven, Kasteelpark 44, 3001 Heverlee, Belgium

Received 9 February 2007; accepted 13 August 2007

Abstract

A combined selective dissolution/quantitative X-ray diffraction (QXRD) approach is proposed for the quantitative mineralogical phase analysis of hydraulic limes. The proposed methodology is validated by the analysis of two model mixtures. Afterwards two commercial hydraulic binders and one self-burned hydraulic quicklime were analysed. Chemical, thermal and microprobe analyses were performed to check the results. It is shown that the proposed selective dissolution/QXRD approach yields reliable quantitative mineralogical information for hydraulic limes in spite of their complex phase composition and the presence of amorphous material.

Keywords: Amorphous material; Characterisation; Thermal analysis; X-ray diffraction; Hydraulic limes

1. Introduction

Quantitative X-ray diffraction has been mainly directed towards applications concerning Portland cement and other common cement types [1–6]. However, there is a renewed interest in hydraulic limes and natural cements because of their use in the restoration of historic buildings [7]. The hydraulic properties of these limes cannot be accurately estimated from the chemical analyses alone [8]. Moreover it seems that the mineralogy cannot be simply predicted from the overall chemistry of the limestone and the associated raw materials [9]. Even more than for cement production, the mineralogy of the limes depends on the nature of the limestone, the burning conditions, the type of kiln used, etc. The amount and nature of the constituent phases of a material is of utmost importance when trying to understand its properties. For this reason and because of the need for quality control in modern production [1], the importance of X-ray diffraction for quantitative phase analysis of these hydraulic binders is apparent [10]. Moreover, minor phases present in some limes may indicate a unique source-rock or source-area. Such information is invaluable in provenance studies where the origin of the binder must be retraced.

In the cement industry, the usual way of quantifying clinker compositions is by using the Bogue calculation [11] or by means of microscopic methods [12]. Since a fundamental assumption of the first method is the requirement of thermodynamic equilibrium conditions—not usually met during clinker production [5,13], the results are not always reliable. In the production of hydraulic limes, sintering/equilibrium conditions are only attained occasionally. The Bogue calculation cannot therefore be applied. Microscopic methods are also used for the determination of clinker/cement composition. Both optical and electron microscopy, often combined with Image Analysis techniques, have been shown to give good results [14,15]. However, microscopy is probably more operator/equipment dependent [16].

Early critical results concerning the quantification of mineral phases showed that 'neither the Bogue, nor the X-ray diffraction methods gave accurate analyses of the cement' [17]. However, efforts have since been made to make X-ray diffraction a suitable technique for the quantification of cement phases [18,19]. Since cement mineralogy is to some extent similar to that of other calcareous hydraulic binders, the Rietveld method has been chosen for quantification in this study. However, most

* Corresponding author. Tel.: +32 16 327586; fax: +32 16 327981.
E-mail address: Gilles.Mertens@geo.kuleuven.be (G. Mertens).

0008-8846/$ - see front matter © 2007 Elsevier Ltd. All rights reserved.
doi:10.1016/j.cemconres.2007.08.002

phases in hydraulic limes and natural cements are only present in small amounts. In the bulk sample, the resolution of XRD is insufficient to accurately identify these minor phases. Selective dissolution techniques have previously been used to characterise major phases in cements [20]. In this work, selective dissolution is proposed as a method of enriching certain phases before quantification. This approach is evaluated by using model mixtures made from pure standard minerals. Moreover, quantitative results are compared with those obtained by thermal analysis techniques. Phase identification was assisted by microprobe analysis.

2. Experimental procedure

2.1. Materials

This study concerns the quantification of three different products, namely a commercial natural hydraulic lime (NHL 2, EN 459-1 [21]), a self-burned hydraulic quicklime and a commercial quick setting natural cement (Ciment Prompt). The self-burned hydraulic quicklime, prepared from the same source-rock as the natural hydraulic lime, was burned for 5 h at 1000 °C in an electric furnace. The samples are listed in Table 1 together with their Cementation Index (CI).

Beside these three products, two model mixtures (M1 and M2) were prepared from pure phases. The compositions of these model mixtures correspond to that of a hydraulic quicklime and a slaked hydraulic lime respectively. These pure phases were synthesised from powder mixtures of CaO (obtained from $CaCO_3$), MgO, Al_2O_3, Fe_2O_3 (all PROLABO purity) and SiO_2 (Aerosil 200®) mixed in suitable proportions. Each powder mixture was thoroughly blended in a Turbula mixer and compressed at 400 bars in a metallic mould. The bricks so obtained were sintered at the appropriate temperature in Pt crucibles and ground in a ring mortar. Phases were sintered at least twice. 3% of the B_2O_3 was added to the C_2S-mixture to stabilise the β-form [22]. The purity of all phases was checked by X-ray diffraction using an internal standard to verify for possible amorphous phases.

2.2. Equipment

Phase identification and quantification was based on powder diffraction patterns recorded with a Philips PW 1830 diffractometer in the Bragg–Brentano geometry equipped with a graphite monochromator and a gas proportional detector. Scans were collected using CuKα radiation in the range 5–75°2θ. Counting time was 3 s for each 0.02°2θ step. Even though "the content of true glass is usually small" in cements [23], the presence of amorphous phases in hydraulic binders cannot be excluded a priori [10]. Therefore, crystalline Si powder (Alfa Aesar®) has been added as an internal standard. It allows quantification of the amorphous content.

The quantification was performed by the Rietveld method with the TOPAS® Academic (TA) Software [24] using the Fundamental Parameters Approach (FPA). In this approach, which leads to stable refinements and physically meaningful information such as crystallite sizes [12], profile shapes are characterised in terms of the physical parameters describing the diffractometer and the diffraction process [25]. Even though samples were prepared using side-loading, the preferred orientation of some phases could not be avoided but was corrected by the use of spherical harmonics.

The chemical composition of the samples was determined by ICP-AES. Samples were mixed with a lithium metaborate/tetraborate flux and fused in an induction furnace. The melt was immediately poured into 5% nitric acid and mixed continuously until complete dissolution. Solutions were analysed with a Spectro Ciros ICP. The SO_4 content was determined by IR analysis, using an Eltra C/S 800 equipment.

TG analyses were performed with a STA 409PC Luxx Netzsch instrument in the range 25–1000 °C. Heating took place at 10 °C/min in alumina crucibles in an inert helium atmosphere (60 ml/min). Gases evolved during analysis were identified with a coupled Netzsch Aëolos mass spectrometer (MS).

Microprobe analyses were performed on Carbon-coated polished sections of powders fixed in a cold setting embedding resin (epofix™). A Jeol Superprobe 733 with an acceleration voltage of 20 kV and a beam intensity of $1.5.10^{-8}$ A was used for semi-quantitative EDX point analyses.

2.3. Methodology

In the first instance, X-ray diffraction patterns were recorded of all samples mixed with the internal standard (10%). They were ground in hexane with a McCrone micronising mill for 5 min. Initially methanol had been used, but its reaction with CaO prevents its use as a grinding agent for quicklimes. These measurements allow all major phases to be quantified. Hydraulic lime and particularly quicklime are easily hydrated. Therefore, all samples were mixed with the standard immediately after preparation or after opening their packaging. XRD measurements were done directly after the evaporation of hexane.

Since most phases are only present in small amounts (<3% weight), each sample was treated in three different ways to concentrate these minor phases. Separation techniques rely either on physical or on chemical properties [26]. However, the complex intermixing of the phases in these binders makes separation based on a physical property alone virtually impossible. Three chemical dissolution techniques were therefore used. The first method relies on the difference in basicity of the minerals [27–29]. 10 g of sample and 0.5 g of

Table 1
Overview of the samples

Sample	Type	CI	Boynton [21] classification
1	Commercial natural hydraulic lime (NHL 2)	0.61	Moderately hydraulic
2	Self-burned hydraulic quicklime	0.38	Weakly hydraulic
3	Commercial quick setting natural cement (Ciment Prompt)	0.98	Eminently hydraulic
M1	Model mixture (hydraulic quicklime)	0.32	Weakly hydraulic
M2	Model mixture (hydraulic lime)	1.10	Eminently hydraulic

Table 2
Chemical compositions of samples 1, 2, 3, M1 and M2 (in wt.% unless otherwise indicated)

Oxides	1	1′	2	2′	3	3′	M1	M2
SiO_2	11.49	9.86	10.06	9.96	16.66	13.36	8.56	22.04[a]
Al_2O_3	2.74	2.26	2.56	2.42	6.2	4.86	3.41	2.00
Fe_2O_3	1.12	0.48	1.21	1.10	3.06	1.65	0.82	0.33
TiO_2	0.095		0.083		0.257			
CaO	56.12	59.95	80.67	76.63	51.76	42.60	84.66	56.70
MgO	2.22	1.39	2.74	2.50	3.36	2.74	2.00	1.00
Na_2O	0.17		0.19		1.95			
K_2O	0.99	0.17	0.77		1.17			
P_2O_5	0.1	0.23	0.43	0.53	0.03			
Ba (ppm)	272	360	1653	2680	248			
Sr (ppm)	489		537		1136			
SO_4	0.3		0.2		4.3			
LOI	24.00		0		10.8		0.00	17.54
Total	99.42		99.14		99.69		99.45	99.61

1′, 2′ and 3′ are calculated from the mineralogy (see further).
[a] This value includes the SiO_2 of the amorphous fraction (15%).

crystalline silicon standard were put in a solution of 35 g of salicylic acid in 250 ml methanol. This treatment concentrates mainly the calcium aluminates [23, pp.150–151]. After 1 h magnetic stirring, the suspension was centrifuged at 3000 rpm for 30 min. The second method consisted of placing 10 g sample and 0.5 g of crystalline silicon standard in a solution of 50 g saccharose in 500 ml H_2O. This treatment concentrates the calcium silicates [9]. After magnetic stirring for 15 min, the suspension was centrifuged at 3000 rpm for 30 min. The last step consisted of treating 10 g of sample and 0.5 g of crystalline Silicon standard with 1 M HCl. This concentrates all acid insoluble phases. After magnetic stirring for 1 h, the suspension was centrifuged at 3000 rpm for 30 min. All three procedures were repeated once on the residues. After drying at 100 °C, the residues were ground in an agate mortar and X-ray diffraction patterns were recorded.

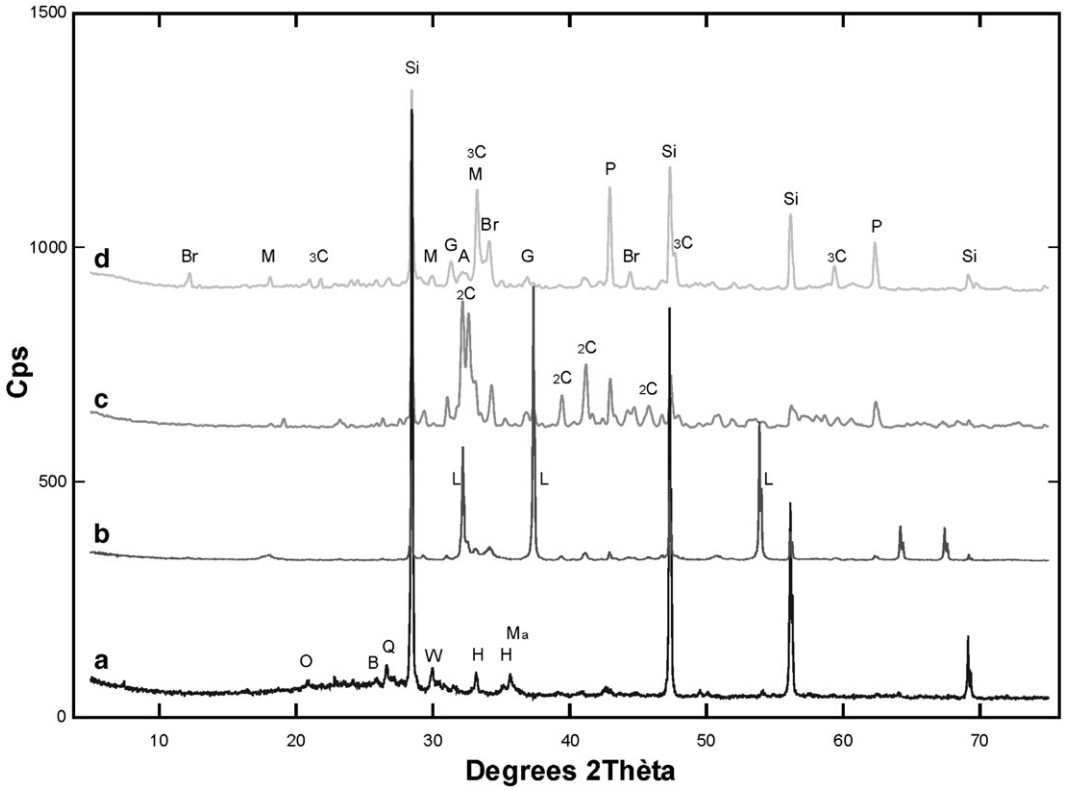

Fig. 1. X-ray diffraction patterns of sample 2. a) after HCl dissolution b) untreated sample c) after treatment with saccharose d) after treatment with salicylic acid. (Si: Silicon, 3C: C_3A, M: $C_{12}A_7$, P: periclase, Br: C_4AF, G: gehlenite, A: apatite, 2C: C_2S, L: lime, Ma: magnetite, H: hematite, W: wollastonite, Q: quartz, O: orthoclase, B: barite).

3. Results and discussion

Table 2 shows the results of the chemical analyses of the three unknown samples and also those of the two model mixtures which were calculated from their known mineralogical compositions.

For each sample four different X-ray diffraction patterns were recorded; one of the untreated sample and three after selective dissolution. The four measurements of sample 2 are shown in Fig. 1. From this figure it is clear that selective dissolution allows identification of phases that show poorly in the pattern of the untreated sample. This is not only because of their limited concentrations but is also due to peak overlap. In the region 30–36°2θ, peaks of lime, portlandite and C_2S dominate the pattern. Diffraction peaks of apatite, hematite, $C_{12}A7$, C_3A, C_4AF, etc. could therefore be overlooked.

All patterns were refined with the Rietveld method. The internal standard enables the quantification of each phase in these patterns. However, some phases were partly or entirely dissolved during the chemical treatment. Entirely dissolved phases are not used in the refinements. The calculated weight fraction of each phase is directly related to the concentration in the original sample by the use of the unreactive internal standard. The results of the refinements for sample 2 are shown in Table 3. From this table it is clear that the dissolution treatments concentrate principally the minor phases. In particular, the salicylic acid treatment concentrates the aluminates by a factor of about 8.5 compared to the untreated sample. Moreover, peak overlap with other minerals is considerably reduced (Fig. 1). Quantifications by the Rietveld method are based not on single peaks but on whole patterns. Nevertheless, reducing peak overlap has a beneficial effect on the refinements. Finally, all results are assembled to give the actual phase concentrations in the original sample. The quantity of lime is determined from the untreated sample, that of the calcium silicates from the saccharose-treated sample, that of the acid insoluble phases from the HCl-treated sample and those of all other phases from the sample treated with salicylic acid. The quantitative results of the two other samples are listed in Table 4.

To validate the combined selective dissolution—QXRD approach, two model mixtures were prepared from pure standard minerals. They were analysed in the same way as the three unknown samples. The results are assembled in Table 5, along with the actual phase concentrations. The “final results” of the Rietveld refinement are obtained from the combined data of the four refinements. The cumulative errors of the “final results” are 4.1% and 5.6% for samples M1 and M2 respectively. These are much lower than the cumulative errors,

Table 3
Results of the Rietveld refinements of sample 2 (numbers in wt.%) and parameters of fit

Phase	Untreated	Salicylic acid	Saccharose	HCl	Final result
Lime	54.9	n/a	n/a	n/a	54.9
C_2AS	0.9	1.2	0.9	n/a	1.2
C_3A	3.4	2.5	1.3	n/a	2.5
$C_{12}A_7$	0.6	0.8	0.3	n/a	0.8
C_4AF	3.2	2.9	0.9	n/a	2.9
Periclase	1.5	2.5	3.2	n/a	2.5
Wollastonite	0.4	0.5	0.3	0.1	0.5
Apatite	0.3	0.5	1.4	n/a	0.5
β-C_2S	20.3	0.0	24.8	n/a	24.8
γ-C_2S	0.3	0.0	1.9	n/a	1.9
Quartz	0.0	0.1	0.1	0.1	0.1
Orthoclase	0.0	0.1	0.1	0.2	0.2
Barite	0.3	0.2	0.0	0.05	0.05
Hematite	0.2	0.1	0.1	0.1	0.1
Magnetite	0.0	0.0	0.0	0.1	0.1
Total	86.3	10.9	35	0.55	93.05
R_{wp}/GoF	16.2/1.54	13.9/1.44	17.9/1.71	13.8/1.54	n/a

Table 4
Final results of the Rietveld refinements of samples 1 and 3 (numbers in wt.%)

Phase	1	3
Calcite	17.8	16.8
Portlandite	42.8	5.8
Spurrite	n/a	3.4
C_2AS	2.3	3.2
C_3A	2.3	1.7
$C_{12}A_7$	0.3	1.7
C_4AF	1.0	4.3
Periclase	1.4	2.7
Wollastonite	0.3	n/a
Apatite	1.3	n/a
Anhydrite	n/a	1.2
Yeelimite	n/a	1.8
β-C_2S	19.5	26.1
γ-C_2S	1.7	3.3
C_3S	n/a	1.9
Quartz	1.2	1.3
Orthoclase	1.0	n/a
Barite	0.1	n/a
Hematite	0.1	0.2
Magnetite	0.1	n/a
Total	93,2	75.4

Table 5
Actual composition of model mixtures M1 and M2 compared with the results from the Rietveld analyses (obtained from the combined data set: ‘final’) and those obtained from the untreated sample only (numbers in wt.%)

Phase	M1 (actual)	M1 (final)	M1 (untreated only)	M2 (actual)	M2 (final)	M2 (untreated only)
Lime	67	67	67	n/a	n/a	n/a
Calcite	n/a	n/a	n/a	15	13.7	13.7
Portlandite	n/a	n/a	n/a	45	46.8	46.8
β-C_2S	18	16.7	16	13	13.1	13.9
C_3A	5	4.8	6.3	2.5	2.5	2.7
C_4AF	2.5	1.0	0.7	1	1.0	0
Wollastonite	2	1.8	2.4	0.3	0.3	0.9
Periclase	2	1.8	1.4	1	0.8	1.4
C_2AS	2	1.9	1.3	2	2.3	0.9
Quartz	1	1.5	3.0	1	1.5	2.7
$C_{12}A_7$	0.5	0.5	0.6	0.2	0.2	0.3
C_3S	n/a	n/a	n/a	4	3.9	3.7
Amorphous	n/a	n/a	n/a	15	13.9	13.1
Cumm. Error		4.1	8.8		5.6	11.1

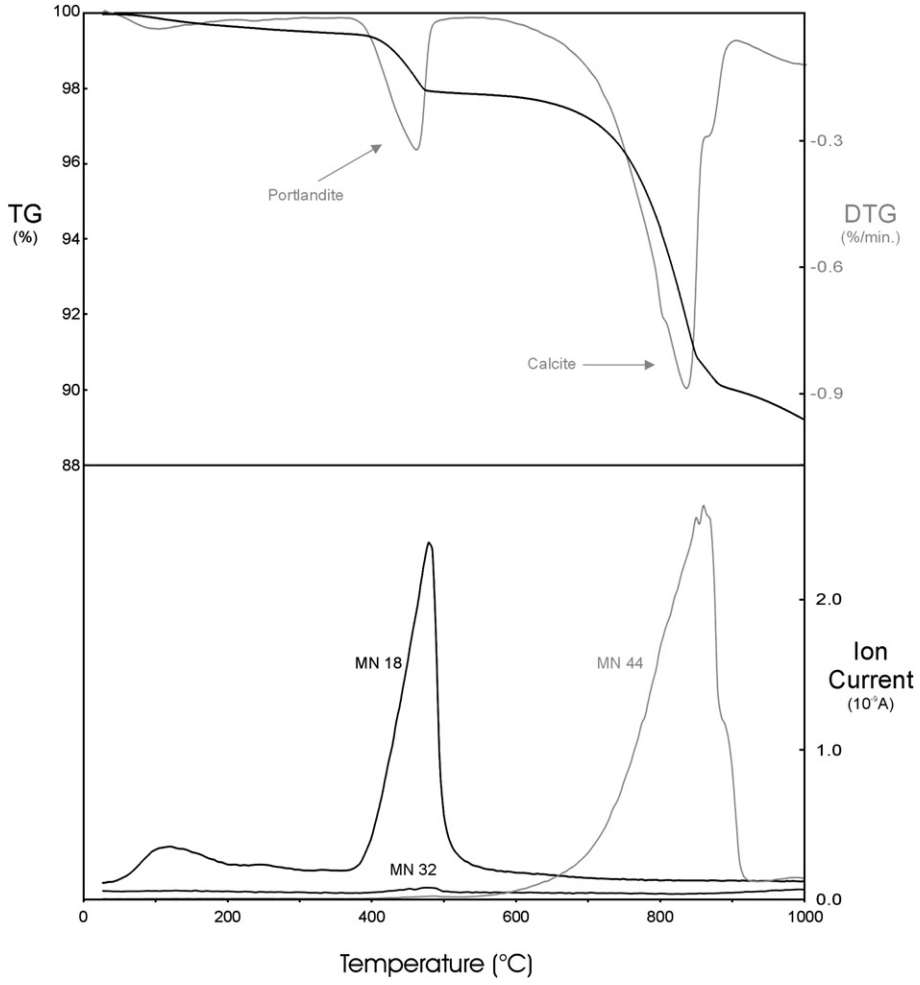

Fig. 2. (upper part) Thermal analysis curves of sample 3 showing the weight loss of portlandite and calcite on the DTG-curves and (lower part) measured ion current at the mass spectrometer for mass number (MN) 18 (H_2O^+), 32 (S^+) and 44 (CO_2^+).

8.8 and 11.1 respectively, obtained by quantifying the diffraction patterns of the untreated samples only. The better correspondance obtained by the selective dissolution approach is explained by the higher concentration of the minerals after treatment of the sample. Their higher concentrations lead to a better resolution of the peaks in the diffraction pattern. This makes unambiguous phase identification possible, as well as a more accurate quantification due to a reduced peak overlap. Raising the concentration of the minor phases by selective dissolution is seen to improve the results.

For the unknown samples, no comparison can be made with the actual phase composition, since these are unknown. However, a comparison of the chemical composition of the samples with that calculated from their mineralogy can be made. There are two limitations to this approach. Firstly, only theoretical mineral compositions can be used. Solid solutions are therefore not taken into account. Secondly, the amorphous part cannot be considered in the calculations. The calculated chemical compositions are given in Table 2 along with the actual chemical composition of the samples. For samples 1 and 2 the agreement is good. For the minor elements, the relative difference between the calculated and the actual composition is higher compared to the difference for the major elements. This is normal, since an even limited substitution of a minor element can lead to a considerable relative increase in its concentration. A similar substitution of a major element will not have an important influence on its concentration relative to the concentration calculated from the major phases in which it is present. In sample 3 all oxides are systematically underestimated. This is due to the large amount of amorphous material of which the composition is variable and unknown.

Table 6
TG-determined CO_2 and H_2O contents expressed as calcite and portlandite respectively

	Portlandite (TGA)	Portlandite (QXRD)	Calcite (TGA)	Calcite (QXRD)
1	40.95	42.8	18.30	17.8
3	6.99	5.8	18.44	16.8
M1	44.68	45[a]	16.03	15[a]

Results are compared with the respective amounts as determined by QXRD. Amounts are in wt.%.
[a] Actual concentration in the model mixture.

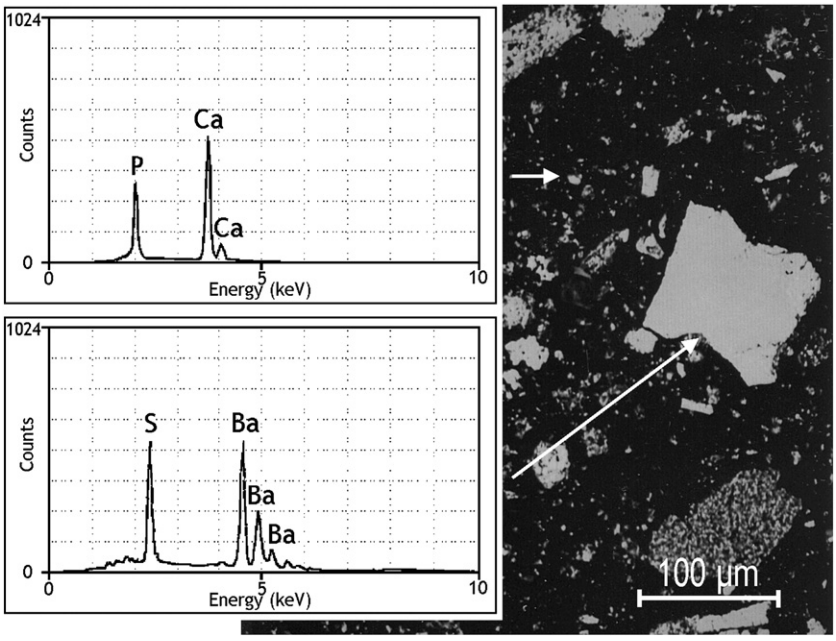

Fig. 3. BSE image of sample 1. The arrows indicate particles of (a) apatite and (b) barite with their corresponding EDX-analyses.

Possible substitutions in major or minor mineral phases enhance these differences.

TG analyses are also helpful for quantifying calcite and portlandite based on their weight loss on decomposition. Fig. 2 shows the TG/DTG/MS curves of sample 3. Even if the weight loss of portlandite and calcite can be clearly recognised on the DTG patterns, it is difficult to delineate the exact temperature range in which it occurs. The complex phase composition of the hydraulic binders adds to the complexity of the patterns. The evolved gas analysis helps in delineating these zones. However, different gases may be released simultaneously upon heating. Fig. 2 shows that around 450 °C, particles with mass number 18 (H_2O^+) and particles with mass number 32 (S^+) are released simultaneously from sample 3. Nevertheless, concentrations of calcite and portlandite were calculated from their estimated weight loss. These are presented in Table 6. The correspondance between the results from the thermal analysis and those from the QXRD is acceptable, considering the limitations of both methods.

From a qualitative point of view, the presence of minor phases was verified by microprobe analyses on the embedded powders of the untreated samples. Fig. 3 shows a BSE image of sample 1 with EDX point analyses of apatite and barite.

The microprobe analyses further revealed that potassium is sometimes incorporated in the dicalcium silicate phase. This may be the reason for the stabilisation of the β-form [22].

4. Conclusions

A combined selective dissolution/quantitative X-ray diffraction approach is proposed as a method of quantifying both slaked and unslaked hydraulic binders. Three different selective dissolution techniques were applied to two commercial hydraulic binders and one self-made hydraulic quicklime. Diffraction patterns of the residues and the untreated samples, mixed with an internal standard, were recorded and quantified by using the Rietveld method. The combined results lead to the composition of both major and minor phases. The chemical composition of these binders was compared with that calculated from their mineralogy. Calculated weight percentages of calcite and portlandite were compared with those obtained by thermal analyses and agree reasonably.

To further validate the proposed methodology, model mixtures were prepared from pure phases and the same approach was applied to obtain quantitative phase results. The results of this combined selective dissolution/QXRD approach were more accurate than those obtained by only quantifying the untreated sample. Moreover, minor phases are more easily identified/quantified after use of the selective dissolution techniques.

The methodology is useful in the field of restoration of historic buildings. The compatibility of restoration mortars and original mortars is a great concern of conservators [8]. Not only chemical, but also mineralogical and physical properties determine compatibility. The accurate characterisation of binders used in restoration mortars covers one aspect of this issue. Since ancient mortars show a broad range in binder compositions [29], a good selection method for binders used in restoration mortars is required. The results of the proposed approach are suitable to provide accurate phase information of such binders.

Acknowledgement

The first author is an Aspirant of the Flemish Fund for Scientific Research (FWO).

References

[1] J.C. Taylor, L.P. Aldridge, Full-profile Rietveld quantitative XRD analysis of Portland cement: standard XRD profiles for the major phase tricalcium silicate (C_3S: 3CaO.SiO_2), Powder Diffr. 8 (1993) 138–1441.

[2] J.C. Taylor, L.P. Aldridge, Phase analysis of Portland cement by full profile standardless quantitative X-ray diffraction—accuracy and precision, Adv. X-ray Anal. 36 (1993) 309–314.

[3] H. Moller, Standardless quantitative phase analysis of Portland cement clinkers, World Cem. (1995) 75–84 September.

[4] R. Berliner, C. Ball, P.B. West, Neutron powder diffraction investigation of model cement compounds, Cem. Concr. Res. 27 (1997) 551–575.

[5] F. Guirado, S. Galí, S. Chinchón, Quantitative Rietveld analysis of aluminous cement clinker phases, Cem. Concr. Res. 30 (2000) 1023–1029.

[6] L. Gobbo, L. Sant'Agostino, L. Garcez, C_3A related polymorphs related to industrial clinker alkalies content, Cem. Concr. Res. 34 (2004) 657–664.

[7] P. Maravelaki-Kalaitzaki, A. Bakolas, I. Karatasios, V. Kilikoglou, Hydraulic lime mortars for the restoration of historic masonry in Crete, Cem. Concr. Res. 35 (2005) 1577–1586.

[8] K. Callebaut, J. Elsen, K. Van Balen, W. Viaene, Nineteenth century hydraulic restoration mortars in the Saint Michael's church (Leuven, Belgium) Natural hydraulic lime or cement ? Cem. Concr. Res. 31 (2001) 397–403.

[9] A. Bernard, J. Millet, R. Hommey, A. Pointdefert, Influence de la température de cuisson et de la nature du calcaire sur la minéralogie des chaux vives, Bull. Liaison Labo. P. et Ch. 79 (1975) 45–50 Sept/Oct.

[10] A.F. Gualtieri, A. Viani, C. Montanari, Quantitative phase analysis of hydraulic limes using the Rietveld method, Cem. Concr. Res. 36 (2006) 401–406.

[11] R.H. Bogue, Calculation of compounds in Portland cement, Ind. Eng. Chem. Anal. Ed. 1 (1929) 192–197.

[12] T. Füllmann, H. Pöllmann, G. Walenta, M. Gimenez, C. Lauzon, S. Hagopian-Babikian, T. Dalrymple, P. Noon, Analytical methods, Int. Cem. Rev. (2001) 41–43 January.

[13] H.G. Midgley, D. Rosaman, K.E. Fletcher, X-ray diffraction examination of Portland cement clinker, Proceedings of the Fourth International Symposium on the Chemistry of Cement, vol. 2, U.S. Government Printing Office, Washington, 1962, pp. 69–74.

[14] V. Furlan, R. Pancella, Examen microscopique en lumière réfléchie de ciments, bétons et mortiers, Chantiers/Suisse 13 (1982) 25–30.

[15] K. Scrivener, H.H. Patel, P.L. Pratt, L.J. Parrott, Analysis of phases in cement paste using backscattered electron images, methanol adsorption and thermogravimetric analysis, Microstructural development during the hydration of cement, Proc. Mater. Res. Soc. Symp. 85 (1987) 67–76.

[16] T. Westphal, G. Walenta, T. Füllmann, M. Gimenez, E. Bermejo, K. Scrivener, H. Pöllmann, Characterisation of cementitious materials, Int. Cem. Rev. (2002) 47–51 July.

[17] L.P. Aldridge, Accuracy and precision of phase analysis in Portland cement by Bogue, microscopic and X-ray diffraction methods, Cem. Concr. Res. 12 (1982) 381–398.

[18] L. Redler, Quantitative X-ray diffraction analysis of high alumina cements, Cem. Concr. Res. 21 (1991) 873–884.

[19] D.L. Bish, S.A. Howard, Quantitative phase analysis using the Rietveld method, J. Appl. Crystallogr. 21 (1988) 86–91.

[20] G. Patiño, A. Viveros, M.I. Avila, Procedures for quantitative X-ray diffraction Portland cement clinker analysis, Proceedings of the Seventeenth International Conference on Cement Microscopy, Calgary, Alberta, 1995, pp. 71–81.

[21] EN 459-1, Building Lime—Part 1: Definitions, Specifications and Conformity Criteria, 2002.

[22] Y.-M. Kim, S.-H. Hong, Influence of minor ions on the stability and hydration rates of β-dicalium silicate, J. Am. Ceram. Soc. 87 (2004) 900–905.

[23] F.M. Lea, in: P.C. Hewlett (Ed.), The Chemistry of Cement and Concrete, 4th Edition, 1998.

[24] A.A. Coelho, TOPAS-Academic; A Computer Programme for Rietveld Analysis, 2004 http://members.optusnet.com.au/~alancoelho/.

[25] R.W. Cheary, A.A. Coelho, A fundamental parameters approach of X-ray line-profile fitting, J. Appl. Crystallogr. 25 (1992) 109–121.

[26] W.A. Gutteridge, On the dissolution of the interstitial phases in Portland cement, Cem. Concr. Res. 9 (1979) 319–324.

[27] S. Takashima, Systematic dissolution of calcium silicate in commercial Portland cement by organic acid solution, Review on the 12th General meeting held in Tokyo, Japan Cement Engineering Association, 1958, pp. 12–13.

[28] K. Van Balen, E.E. Toumbakari, M.T. Blanco-Varela, J. Aguilera, F. Puertas, A. Palomo, C. Sabbioni, C. Riontino, G. Zappia, Environmental Deterioration of Ancient and Modern Hydraulic Mortars, 2002 EDAMM project ENV4-CT95-0096.

[29] J. Elsen, Microscopy of historic mortars—a review, Cem. Concr. Res. 36 (2006) 1416–1424.